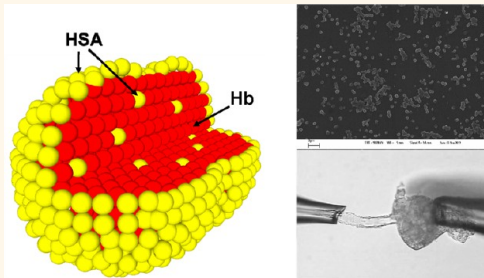


# Nonvasoconstrictive Hemoglobin Particles as Oxygen Carriers

Yu Xiong,<sup>†,\*</sup> Zhi Zhao Liu,<sup>‡</sup> Radostina Georgieva,<sup>†,§</sup> Kathrin Smuda,<sup>†</sup> Axel Steffen,<sup>†</sup> Mauricio Sendeski,<sup>‡</sup> Andreas Voigt,<sup>†</sup> Andreas Patzak,<sup>‡</sup> and Hans Bäumler<sup>†,\*</sup>

<sup>†</sup>Institute of Transfusion Medicine and Berlin-Brandenburg Center for Regenerative Therapies, Charité-Universitätsmedizin Berlin, Charitéplatz 1, 10117 Berlin, Germany, <sup>‡</sup>Institute of Vegetative Physiology, Charité-Universitätsmedizin Berlin, Charitéplatz 1, 10117 Berlin, Germany, and <sup>§</sup>Department of Medical Physics, Biophysics and Radiology, Medical Faculty, Trakia University, ul. "Armeiska" 11, 6000 Stara Zagora, Bulgaria

**ABSTRACT** Artificial oxygen carriers, favorably hemoglobin-based oxygen carriers (HBOCs), are being investigated intensively during the last 30 years with the aim to develop a universal blood substitute. However, serious side effects mainly caused by vasoconstriction triggered by nitric oxide (NO) scavenging due to penetration of nanosized HBOCs through the endothelial gaps of the capillary walls and/or oxygen oversupply in the precapillary arterioles due to their low oxygen affinity led to failure of clinical trials and FDA disapproval. To avoid these effects, HBOCs with a size between 100 and 1000 nm and high oxygen affinity are needed. Here we present for the first time unique hemoglobin particles (HbPs) of around 700 nm with high oxygen affinity and low immunogenicity using a novel, highly effective, and simple technique. The fabrication procedure provides particles with a narrow size distribution and nearly uniform morphology. The content of hemoglobin (Hb) in the particles corresponded to 80% of the Hb content in native erythrocytes. Furthermore, we demonstrate a successful perfusion of isolated mouse glomeruli with concentrated HbP suspensions *in vitro*. A normal, nonvasoconstrictive behavior of the afferent arterioles is observed, suggesting no oxygen oversupply and limited NO scavenging by these particles, making them a highly promising blood substitute.



**KEYWORDS:** hemoglobin-based oxygen carriers · manganese carbonate · hemoglobin particles · co-precipitation · microperfusion

In Germany and the United States alone approximately 20 million (4.5 million in Germany and 15 million in the U.S.) units of packed red blood cells (RBCs) were transfused in 2008.<sup>1,2</sup> However, transfusions have several limitations: mismatched transfusions despite rigorous typing and cross-matching prior to transfusion, risk of transfusion-related acute lung injury, immunomodulation, hemolytic transfusion reactions, bacterial or viral infections, limited shelf life of blood products, and logistical constraints.<sup>1,3,4</sup> According to the World Health Organization report in 2011, in 39 countries blood donations are still not routinely tested for transfusion-transmissible infections and 47% of the donations in developing countries are tested in laboratories without quality assurance.<sup>5</sup> Hence, there is an urgent need for the development of artificial oxygen carriers without the above-mentioned risks.

Stroma-free hemoglobin cannot be used as a blood substitute due to its short circulation time and nephrotoxicity.<sup>6</sup> In the past decades, diverse modifications of hemoglobin

(Hb) such as intra- and intermolecular cross-linking, macromolecule conjugation, or encapsulation<sup>3,7</sup> have been intensively studied to overcome these problems. However, most of these products cause serious side effects, particularly a hypertension caused by vasoconstriction.<sup>3,4,7</sup> Two major hypotheses about the mechanisms of the vasoconstriction caused by hemoglobin-based oxygen carriers (HBOCs) are currently under discussion: the nitric oxide (NO) scavenging by small HBOCs and the oxygen oversupply caused by HBOCs with low oxygen affinity.<sup>8,9</sup>

NO is produced by the blood vessel endothelial cells and is an important vasodilator, causing relaxation of these vessels and consequently preventing vasoconstriction.<sup>10,11</sup> Stroma-free hemoglobin and nanosized HBOCs can penetrate through the gaps between the endothelial cells and bind the NO released into the smooth muscle tissue. It has been shown that vasoconstriction and hypertension are inversely proportional to the size of the HBOCs.<sup>12,13</sup> Thus, synthesis of larger HBOCs would be helpful to solve the

\* Address correspondence to  
hans.baemler@charite.de (H. Bäumler),  
yu.xiong@charite.de (Y. Xiong).

Received for review April 25, 2013  
and accepted August 3, 2013.

Published online August 05, 2013  
10.1021/nn402073n

© 2013 American Chemical Society

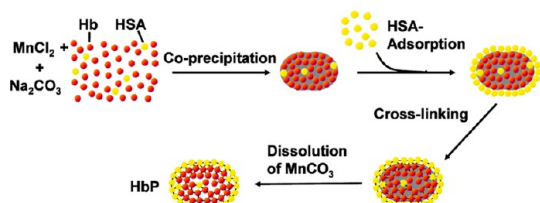
problem of NO scavenging in the vessels. To avoid HBOC extravasation through the endothelial gaps, their diameter should exceed 100 nm. Particles in the size range 1–3  $\mu\text{m}$  can be strongly phagocytosed,<sup>14–16</sup> and particles larger than 5  $\mu\text{m}$  can block microcirculation at higher concentrations. In both cases the shelf life of the particles is reduced. Consequently, the size of HBOCs should be preferably less than 1  $\mu\text{m}$  and more than 100 nm.

The new-generation HBOCs should have a high oxygen affinity to prevent premature release of oxygen in the precapillary arterioles, which would lead to oxygen oversupply and vasoconstriction caused by an autoregulatory mechanism.<sup>9</sup>

The use of carbonates as a template for fabrication of microparticles and microcapsules has currently gained increasing interest due to the high loading capacity of the  $\text{CaCO}_3$  particles and the mild fabrication conditions and biocompatibility.<sup>17–21</sup> In previous studies we synthesized protein microparticles by co-precipitation with  $\text{CaCO}_3$ , followed by protein cross-linking and dissolution of the  $\text{CaCO}_3$  template.<sup>22–24</sup> Here we present unique submicrometer hemoglobin particles (HbPs) as new HBOCs adapting our procedure to the above-mentioned requirements for blood substitutes: particle size below 1  $\mu\text{m}$ , high oxygen affinity, and avoiding vasoconstriction of small blood vessels.

## RESULTS AND DISCUSSION

The synthesis of HbPs is based on co-precipitation of Hb with  $\text{MnCO}_3$  immediately followed by addition of human serum albumin (HSA). HSA adsorbs on the surface of the formed particles and prevents agglomeration. The co-precipitated and adsorbed proteins are then



**Scheme 1.** Fabrication scheme of HbPs.

cross-linked by glutaraldehyde, and the  $\text{MnCO}_3$  template is dissolved, resulting in polymerized submicrometer HbPs (Scheme 1). The HbPs are weakly autofluorescent due to the glutaraldehyde cross-linking<sup>25</sup> and can be detected in the fluorescence channels of the confocal microscope (Figure 1).

Measured by dynamic light scattering, the apparent average size of the HbPs is around  $710 \pm 60$  nm. Observed by scanning electron microscopy (SEM), the particles emerge peanut-shaped (Figure 2a–c). The average longest diameter and shortest diameter of HbPs are  $860 \pm 145$  nm and  $625 \pm 130$  nm, respectively (Figure 2b). The formulation procedure provides a narrow size distribution and almost uniform morphology of the particles independent of the stirring rate during co-precipitation.

The co-precipitation of protein and  $\text{MnCO}_3$  provided a high Hb entrapment efficiency. Typically, a Hb entrapment efficiency of 73% (corresponding to 25.4 mg Hb per 100 mg  $\text{MnCO}_3$ ) can be achieved by precipitation of 0.25 M  $\text{Na}_2\text{CO}_3$  with 0.25 M  $\text{MnCl}_2$  containing 10 mg  $\text{mL}^{-1}$  Hb, which is 35-fold more effective than Hb adsorption on preformed  $\text{MnCO}_3$  particles. One single particle captures at least 35 fg of Hb in a volume of 0.13 fL, if the particle volume is estimated with the prolate spheroid volume formula. For comparison, a human RBC has a volume of approximately 90 fL and contains 30 pg of Hb.<sup>26</sup> Hence, the Hb content in 90 fL of Hb- $\text{MnCO}_3$  particles was 23.7 pg, or 80% of the Hb content of the RBCs. The Hb amount in the  $\text{MnCO}_3$  particles can be even additionally increased by enhancing the initial amount of Hb during co-precipitation. To the best of our knowledge, spontaneous capturing of such high amounts of proteins in nearly uniform submicrometer particles is unique and has not been reported until now. The inorganic compounds are completely removed by dissolution using ethylenediaminetetraacetic acid (EDTA) followed by several washing steps. In particular, ICP-OES (inductively coupled plasma optical emission spectrometry) measurements confirmed the absence of Mn in the HbPs.

One of the most important aspects in the development of HBOCs consists in the minimization of MetHb

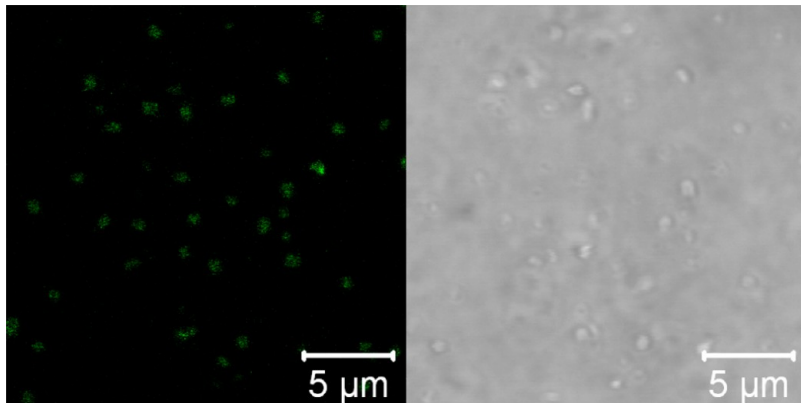


**Figure 1.** Confocal laser scanning micrograph of HbPs in fluorescence mode (left) and transmission mode (right).

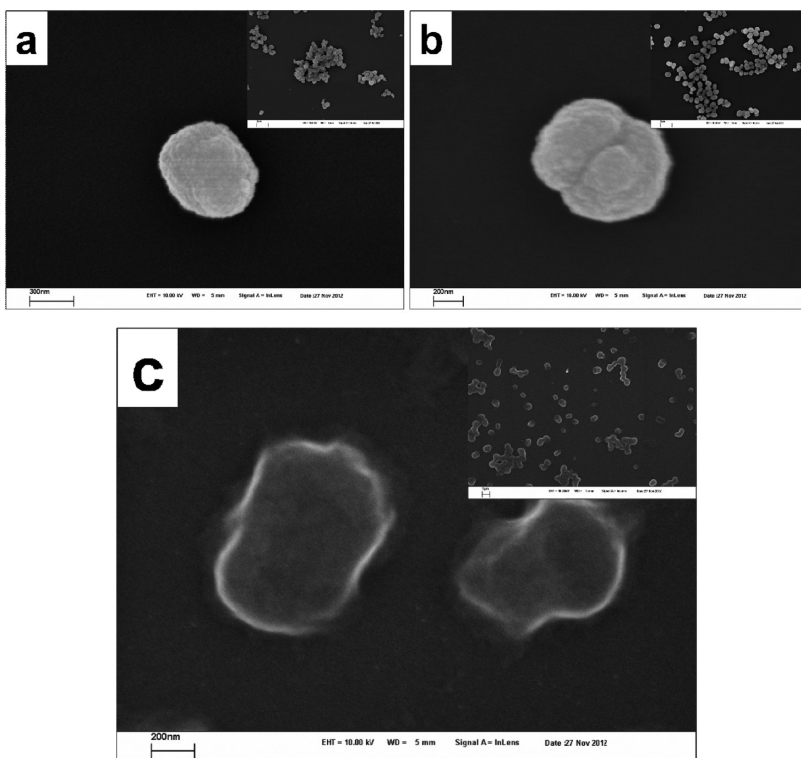


**Figure 2.** SEM images of (a)  $\text{MnCO}_3$  particles (without protein); (b)  $\text{Hb}-\text{MnCO}_3$  hybrid particles after cross-linking; (c) HbPs after  $\text{MnCO}_3$  dissolution. HbPs are shrunken as a result of drying upon sample preparation for SEM measurements. Scale bars: (a) 300 nm, (b) and (c) 200 nm; insets: (a, b) 2  $\mu\text{m}$ , (c) 1  $\mu\text{m}$ .

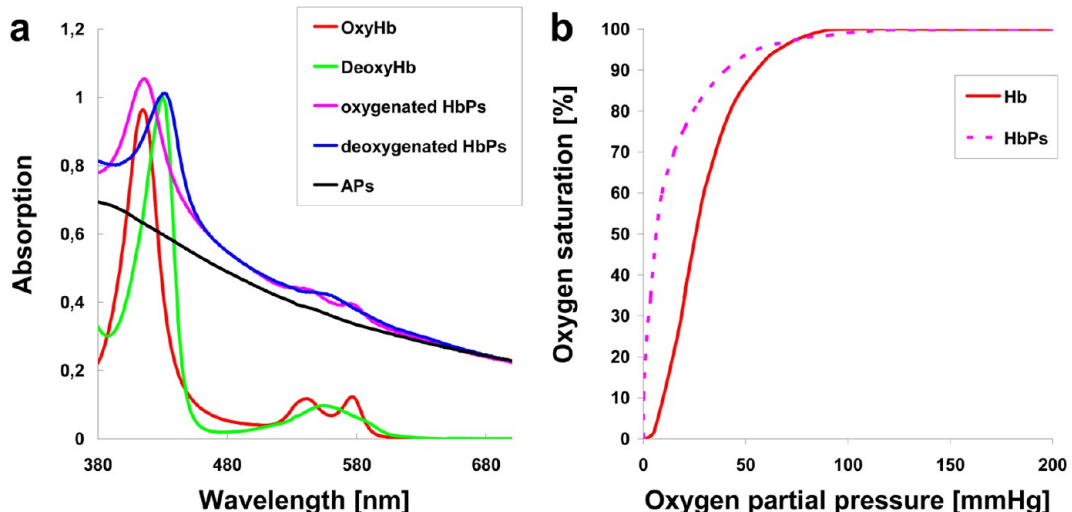


**Figure 3.** Functionality of HbPs. (a) Absorption spectra of oxygenated Hb (OxyHb), deoxygenated Hb (DeoxyHb), oxygenated and deoxygenated HbPs, and APs. The gradual increase in absorption from 700 to 380 nm of HbPs and APs is due to the light scattering of the particles. (b) Oxygen dissociation curves of Hb and HbPs. The  $p_{50}$  values were 26.5 mmHg for Hb solution and 6 mmHg for HbPs, respectively.

formation during the fabrication process since MetHb impairs the ability of the carriers to deliver oxygen to the tissue. Typically, the MetHb concentration in HBOCs should be held below 10%.<sup>27</sup> Applying the protocol described here, we obtained HbP particles with a MetHb concentration of  $10.2 \pm 2.9\%$  as measured immediately after preparation. It was possible to further reduce this value to less than 5% ( $4.9 \pm 2.4\%$ ) by

treatment with ascorbic acid under anaerobic conditions. The last values only little differ from the values measured for the MetHb concentration of the initial Hb solution (in the range from 2% to 4%).

The functionality of the HbPs, their ability to bind and deliver oxygen, was investigated by spectral analysis. Figure 3a presents the absorption spectra of oxygenated and deoxygenated HbPs in comparison

to the corresponding spectra of stroma-free Hb as well as to the absorption spectrum of albumin particles (APs) prepared by the same procedure. Due to light

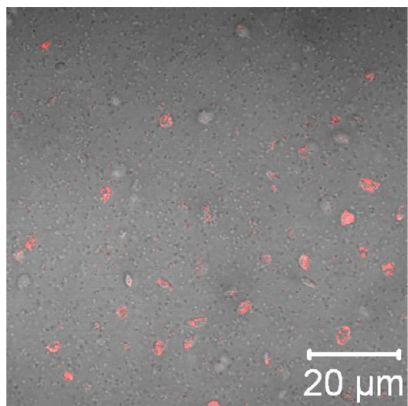


**Figure 4.** CLSM image (overlay of transmission and fluorescence channels) of HbPs and platelets after 45 min incubation in a water bath at 37 °C. The platelets are stained with phycoerythrin (PE)-conjugated mouse anti-human CD41a after incubation. HbPs appear as small dark points in the transmission mode.

scattering the spectra of particles (HbPs and APs) are shifted toward higher absorption values over the whole wavelength interval. However, the typical absorption maxima of oxygenated and deoxygenated Hb are clearly reflected in the respective spectra of HbPs and are absent in the spectrum of APs. The shift of the Soret peak as well as the spectral changes in the region 530–590 nm by oxygenation and deoxygenation confirms the ability of HbPs to bind and release oxygen (Figure 3a). Additionally, the oxygen dissociation curve of HbPs is left-shifted from the dissociation curve of the Hb solution (Figure 3b). The oxygen dissociation curve displays the dependency of Hb oxygen saturation on the partial oxygen pressure in the solution. The value  $p_{50}$  represents the partial pressure at 50% oxygen saturation and serves as a measure for the oxygen affinity. The  $p_{50}$  value of Hb in solution is 26.5 mmHg, and the suspension of HbPs has a  $p_{50}$  of 6 mmHg. Therefore, HbPs have a higher affinity to oxygen. High oxygen affinity (low  $p_{50}$ ) is one of the most important properties of the new-generation HBOCs mentioned above. It is necessary to avoid vasoconstriction after an

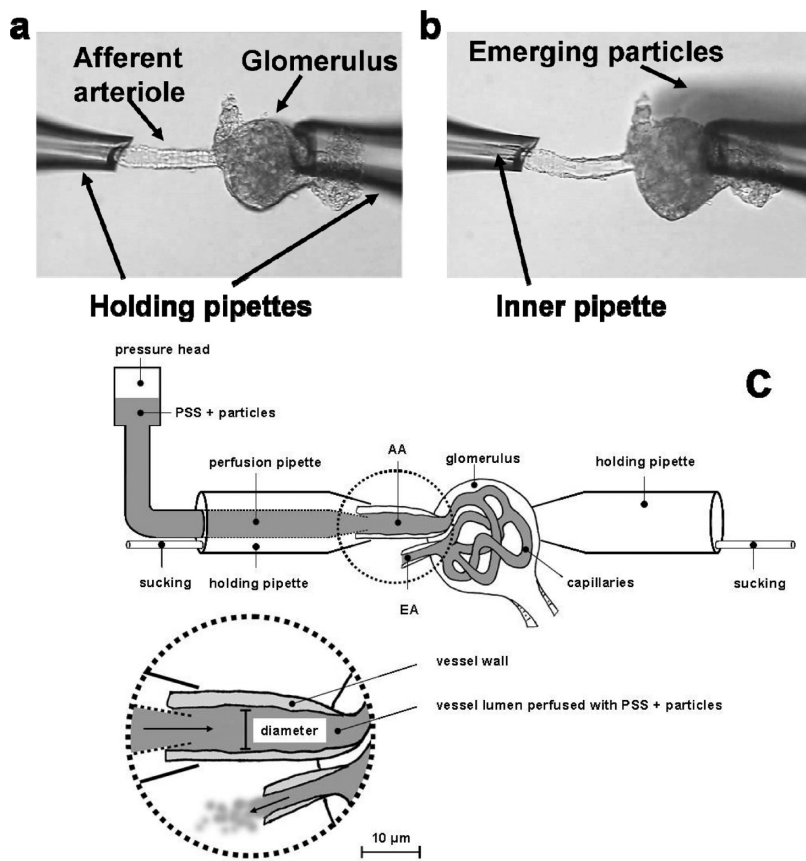


**Figure 5.** Microperfusion of afferent arterioles attached to their glomeruli. Microscope images (a) previous to perfusion; (b) during perfusion with HbPs. Two micropipets hold an attached glomerulus (right) and the free end of an afferent arteriole (left), respectively. An inner pipet inside the left holding pipet is advanced into the lumen of the arterioles. (c) Principle of the perfusion of glomerular arterioles and glomerular capillaries by particles suspended in physiological salt solution (PSS). The afferent arteriole (AA) is sucked into a holding pipet and perfused by an additional smaller perfusion pipet placed within the holding pipet. The solution passes through the glomerular capillaries and leaves the preparation via the efferent arteriole (EA). The whole preparation is placed in a thermocontrolled chamber containing PSS. The changes of the arteriolar diameter were detected by a video system connected to an inverted microscope.

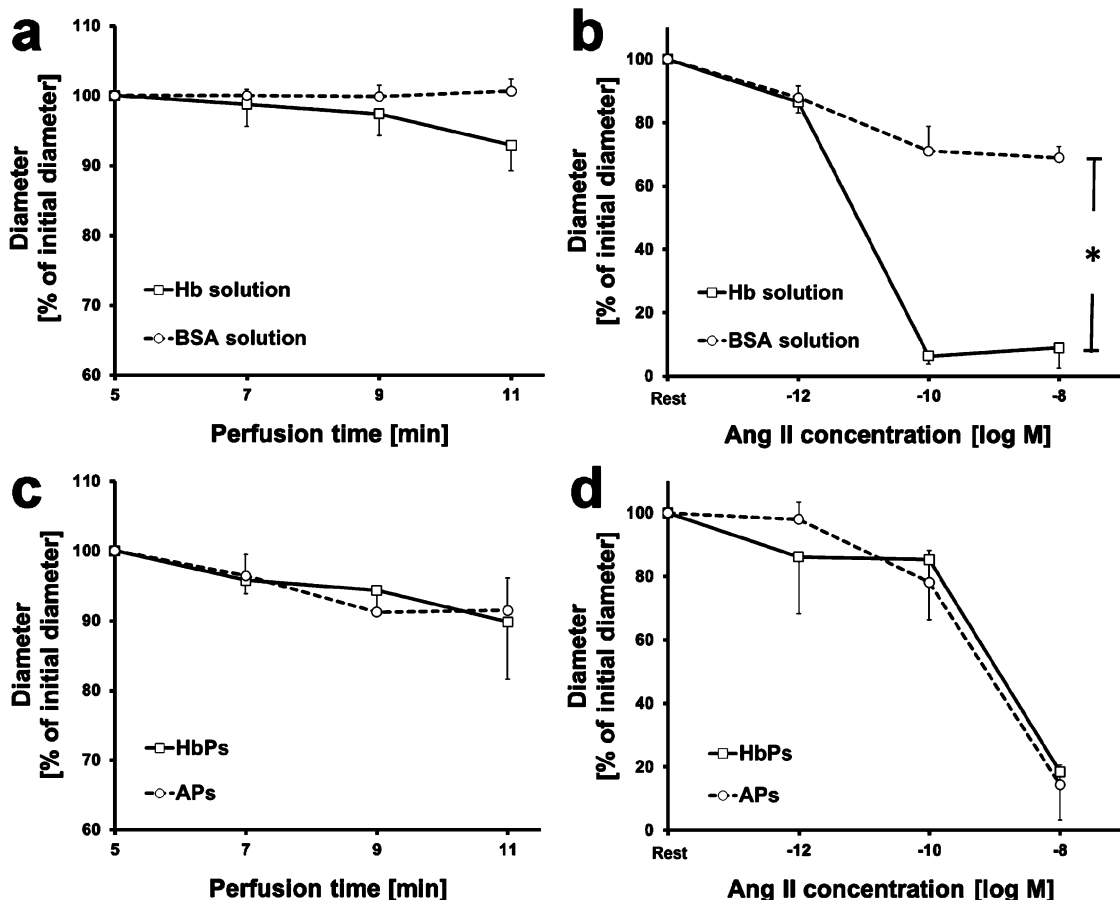


**Figure 6.** Diameter of afferent arterioles in percentage of their initial diameters during perfusion and vessel reactivity to Ang II after perfusion. (a) Arterioles perfused with Hb solution ( $n = 5$ ) and with BSA solution ( $n = 6$ ). The diameters of afferent arterioles after 5 min perfusion (steady state) were chosen as initial diameters. (b) Ang II dose-response curves of afferent arterioles after perfusion with Hb solution ( $n = 5$ ) and with BSA solution ( $n = 6$ ). The diameters immediately before application of Ang II were set as initial diameters. The afferent arteriolar response to Ang II was increased significantly by Hb application, compared with the BSA group ( $p = 0.004$ ). (c) Percentage of the initial diameters from afferent arterioles treated with HbPs ( $n = 6$ ) and APs ( $n = 6$ ) as control. The diameters of afferent arterioles after 5 min perfusion (steady state) were chosen as initial diameters. (d) Ang II dose-response curves of afferent arterioles after perfusion with HbPs ( $n = 6$ ) and with APs ( $n = 6$ ). The diameters immediately before application of Ang II were set as initial diameters. Both particles showed similar effects on afferent arteriolar tone and its reactivity to Ang II. (a–d) Results of afferent arteriolar diameter measurements were expressed as means  $\pm$  standard error of the mean. Here “ $n$ ” represent the number of perfused afferent arterioles.

autoregulatory mechanism caused by oxygen oversupply in the precapillary arterioles.<sup>9</sup> Winslow suggests a  $p50$  of 5–10 mmHg for the new cell-free HBOCs.<sup>9</sup>

To investigate the immunological response to the HbPs, we incubated the HbPs with heparinized whole blood for 30 min at 37 °C and quantified the phagocytic activity of blood leucocytes. Only 3.9% phagocytizing leucocytes were detected, which suggests low immunogenicity of the HbPs. Furthermore, we incubated the HbPs with platelet-rich plasma for 45 min at 37 °C. After incubation, the platelet number did not change compared to the control sample incubated with sterile physiological saline. The activated platelets were also quantified using fluorescein isothiocyanate (FITC) conjugate anti-CD62p and flow cytometry. Only 0.2% activated platelets were found after incubation with the HbPs. This is comparable to the control sample. Also no aggregation of HbPs or platelets after incubation was seen under the microscope (Figure 4). In summary,

no interaction between HbPs and platelets was observed.

The effect of HbPs on the function of microvessels was investigated in several experiments using an *in vitro* model. Afferent arterioles, the microvessels in the kidney just preceding the glomerular capillary network, play a vital role in the regulation of renal blood flow. Their resistance is an essential determinant of the glomerular filtration rate, and they are very sensitive to changes in NO bioavailability.<sup>28</sup> In addition, the vasoconstrictor angiotensin II (Ang II) plays an important role in the control of arteriole diameter constricting afferent arterioles significantly in a dose-dependent manner.<sup>29,30</sup> The vasoreactivity of the arteriole to Ang II also increases with decreasing NO bioavailability.<sup>29–31</sup> So, we perfused isolated afferent arterioles attached to their glomeruli with particles (Figure 5, supporting video 1) and protein solutions for 11 min, respectively. After perfusion, the afferent arterioles were treated with

Ang II in progressive doses to check the vasoreactivity of the vessel to Ang II. The luminal diameters of afferent arterioles in steady state (after 5 min perfusion) were chosen as initial diameters.

At the beginning we measured the influence of pure Hb solution on vessel tone and its vasoreactivity to Ang II (supporting video 2). Bovine serum albumin (BSA) solution with the same concentration served as a control. Hb and BSA did not significantly affect the arteriolar tone during the 11 min perfusion (Figure 6a). Remarkably, the afferent arteriolar response to Ang II was significantly increased by Hb in comparison to the control BSA solution. The diameter of the vessels perfused with Hb solution decreased to  $6.3\% \pm 2.5\%$  of the initial diameter at the maximal constriction dose of Ang II, whereas the same dose induced only a moderate constriction to  $71.0\% \pm 7.7\%$  of the initial diameter in the vessels perfused with BSA (Figure 6b). Hence, Hb exhibited a deleterious effect on afferent arterioles compared to the pure albumin solution. These observations are in agreement with other studies, which showed that stroma-free Hb induces strong vasoconstriction.<sup>8,32,33</sup> Scavenging of NO, a potent physiological vasodilator in the microvessels, is assumed to be the main reason for this constrictor effect.<sup>10,11,28</sup>

In the next step, the influence of HbPs on arteriolar tone and the vasoreactivity of vessels to Ang II after perfusion were investigated (supporting video 3). APs were used as a control for comparison. No significant differences between the behavior of the afferent arterioles perfused with HbPs and APs were found. During perfusion a slight reduction of the size of the vessels

by both particles was observed (Figure 6c). This was probably caused by reduced flow coming out of the pipet into the arteriole due to particle sedimentation inside the pipet since we used a concentrated particle suspension and small-sized inner pipets with a diameter of  $5\ \mu\text{m}$ . Neither the tone of afferent arterioles nor their reactivity to Ang II was affected by HbPs in comparison to the APs (Figure 6c and d). Thus, the NO scavenging of stroma-free Hb was blunted by the construction of HbPs.

## CONCLUSION

In conclusion, we presented HbPs as an enormously promising new type of HBOCs. These HbPs are fabricated by using a novel, simple technique, which exploits the high Hb capture ability of  $\text{MnCO}_3$ , reported here for the first time. The fabrication method provides particles with a narrow size distribution in the submicrometer range and nearly uniform morphology. The HbPs demonstrated here are able to bind and release oxygen. They have a high oxygen affinity, which is necessary to prevent a premature release of oxygen in the precapillary arterioles. Microperfusion experiments showed that concentrated HbP suspensions can easily pass through the glomerulus. Remarkably, the behavior of afferent arterioles perfused with HbPs concerning arteriolar tone and reactivity to Ang II was similar to the behavior of the control group perfused with APs, in contrast to stroma-free Hb solutions, which significantly enhanced the vasoreactivity to Ang II. This finding and the high oxygen affinity are highly promising prerequisites of the new type of HbPs as a candidate for a novel blood substitute.

## EXPERIMENTAL SECTION

**Materials.** Hb was extracted from bovine RBCs by hypotonic hemolysis.<sup>34</sup> Briefly, fresh bovine whole blood (obtained from Schlachtbetrieb GmbH Perleberg, anticoagulated with EDTA) was centrifuged (2500g, 10 min, 4 °C), the packed RBCs were washed three times with ice cold phosphate-buffered saline, and 5 volumes of ice cold Ampuwa (aqua ad injectabilia; Fresenius Kabi Deutschland GmbH) were added to 1 volume of washed RBCs. The solution was stirred at 4 °C overnight and then centrifuged (10000g, 1 h, 4 °C). The supernatant was filtered through a  $0.1\ \mu\text{m}$  polyethersulfone filter (Sartorius AG, Germany) and stored as stock solution at  $-80\ ^\circ\text{C}$  until use.

Bovine serum albumin, FITC-BSA, glutaraldehyde (GA), manganese chloride ( $\text{MnCl}_2$ ) tetrahydrate, sodium carbonate ( $\text{Na}_2\text{CO}_3$ ), phosphate-buffered saline pH 7.4, glycine, and sodium borohydride ( $\text{NaBH}_4$ ) were purchased from Sigma-Aldrich; EDTA and sodium dithionite (SDT) were purchased from Fluka; sodium hydroxide ( $\text{NaOH}$ ) was purchased from Carl Roth; Ampuwa and sterile 0.9% NaCl solution were purchased from Fresenius Kabi Deutschland GmbH. Human albumin solution 20% was purchased from Grifols Deutschland GmbH; mouse anti-human CD41a and CD 62p were purchased from BD Biosciences.

**Preparation of HbPs and APs.** Particles were fabricated in a modified and improved manner based on a novel technique as previously described.<sup>22,23</sup> Briefly, equal volumes of 0.25 M  $\text{Na}_2\text{CO}_3$  and  $\text{MnCl}_2$  containing 10 mg  $\text{mL}^{-1}$  Hb or BSA and 1 mg  $\text{mL}^{-1}$  HSA were rapidly mixed in a beaker under vigorous stirring at room temperature. HSA (weight ratio to Hb or BSA 1:2)

was added, and the suspension was stirred for 5 min. The obtained hybrid particles were separated by centrifugation and washed three times with sterile 0.9% NaCl solution. The particles were suspended in GA solution (0.008%) and incubated at room temperature for 1 h, followed by three washing steps with sterile 0.9% NaCl solution. The remaining GA in the particle suspension was quenched with glycine (mol ratio to initial GA = 40:1). The  $\text{MnCO}_3$  template was removed by treatment of hybrid particles with EDTA solution (0.2 M, pH 7.4), and the particles were reduced with  $\text{NaBH}_4$  (mol ratio to initial GA = 3:1). Finally, the resulting particles were centrifuged, washed three times, and resuspended in sterile 0.9% NaCl solution containing 2% HSA for further use. The co-precipitation, cross-linking, and dissolution steps were carried out under oxygen-free conditions. For phagocytosis assay, the FITC-BSA (weight ratio to Hb = 1:100) was added into the  $\text{MnCl}_2/\text{Hb}$  solution to produce FITC-labeled HbPs.

**Characterization of HbPs.** Concentrations of Hb stock solution and MetHb were determined by the standard cyanomethemoglobin method<sup>35</sup> using a UV-vis spectrophotometer (Hitachi U2800, Hitachi High-Technologies Corporation). The light scattering of the particles was compensated applying the absorption value at 597 nm (isosbestic point for MetHb and cyanomethemoglobin).

Hb entrainment efficiency (EE) of  $\text{MnCO}_3$  particles was determined as the difference between the total Hb amount applied ( $\text{Hb}_t$ ) and the Hb amount determined in the supernatant ( $\text{Hb}_r$ ) after co-precipitation and after each washing step. The EE% was calculated according to the following equation:  $\text{EE\%} = (\text{Hb}_t - \text{Hb}_r) \times 100\%/\text{Hb}_t$ . The measurements were

performed with a microplate reader (PowerWave 340, BioTek Instruments GmbH) at 415 nm.

Residue manganese content in HbPs was measured with ICP-OES (Trace Scan Thermo Jarrell).

Confocal laser scanning microscopy (CLSM) images were taken with an LSM 510 Meta confocal microscope (Carl Zeiss MicroImaging GmbH, Jena, Germany) equipped with a  $100\times$  oil-immersion objective (numerical aperture 1.3) applying an excitation wavelength of 488 nm and a long-pass emission filter of 505 nm.

For SEM analysis, samples were prepared by applying a drop of the particle suspension to a glass slide and then letting the drop dry overnight. Afterward, the samples were sputtered with gold. Measurements were conducted using a Gemini Leo 1550 instrument at an operation voltage of 3 keV.

The particle size was measured from SEM images using ImageJ 1.44p software. Additionally, the particle size was measured by dynamic light scattering using a Zetasizer Nano ZS instrument (Malvern Instruments Ltd, U.K.).

Oxygen dissociation curves were measured by a modified procedure based on the method described by Zhang *et al.*<sup>36</sup> The partial oxygen pressure ( $pO_2$ ) was detected by an oxygen electrode (GMH 3630, Greisinger Electronic GmbH, Germany). In brief, Hb or HbPs were suspended in phosphate buffer (pH 7.4, 0.1 M Cl-1) and were held at 37 °C. The absorption ( $A$ ) at 576, 580, and 588 nm was measured at  $pO_2$  values between 0 mmHg ( $A_{deoxy}$ ) and 160 mmHg ( $A_{oxy}$ ). The absorption at 584 nm (isosbestic point for oxygenated Hb and deoxygenated Hb) was used to exclude evaporation and light scattering. The value of oxygen saturation ( $Y$ ) at a given  $pO_2$  was calculated according to the following equation:  $Y = (A - A_{deoxy})/(A_{oxy} - A_{deoxy})$ . Oxygenation and deoxygenation were operated by gas with air and argon, respectively. A complete deoxygenation of Hb and HbPs was achieved by adding SDT.

The phagocytic activity of leukocytes after addition of FITC-labeled HbPs was measured *in vitro* in human whole blood using a Phagotest kit (Glycotope-Biotechnology GmbH, Heidelberg, Germany) and was quantified by flow cytometry (FACSCanto II, Becton & Dickinson, Franklin Lakes, NJ, USA).

Incubation of the HbPs with platelet-rich plasma (PRP) was performed as follows. The PRP was obtained by centrifugation of citrated whole blood at 140g for 15 min. Then 500  $\mu$ L of PRP was carefully mixed with 100  $\mu$ L of 20% (v/v) HbPs or sterile physiological saline. The mixtures were incubated in a water bath at 37 °C for 45 min. Before and after incubation, the platelet number was detected using an ABX Micros 60 hematology analyzer (Horiba Europe GmbH). Additionally, 50  $\mu$ L mixtures were taken before and after incubation and incubated with PE- or FITC-labeled mouse anti-human CD41a or 62p for 30 min. The treated mixtures were analyzed by flow cytometry and CLSM.

**Microperfusion of Afferent Arterioles with Glomeruli.** Experiments were performed in accordance with the regulations of the Office for Health and Social Matters of Berlin, Germany.

The methods to isolate and microperfuse the afferent arterioles are similar to those described previously.<sup>37</sup> Briefly, male C57BL/6 adult mice (FEM, Charité-Berlin, Germany) were anesthetized with isoflurane (Abbott AG, Baar, Switzerland) and sacrificed by cervical dislocation. Kidneys were removed and sliced along the corticomedullary axis. Afferent arterioles attached to their glomeruli were dissected at 4 °C with sharpened forceps and transferred to a temperature-controlled chamber assembled on the stage of an inverted microscope. Dulbecco's modified Eagle medium (DMEM, Gibco, Darmstadt, Germany) was used for dissection and as bath solution (0.1% albumin). Afferent arterioles were perfused using a set of perfusion pipets handmade from glass tubes (Vestavia Scientific, Vestavia Hills, AL, USA) and assembled on an electronically controlled micromanipulator. Two holding pipets held the free end of an arteriole and of an attached glomerulus, respectively. An inner pipet inside one of the holding pipets was advanced into the lumen of the arterioles, thus providing flow to the arteriolar lumen. To provide a physiological flow in the afferent arterioles, the pressure in the pressure head was set to 100 mmHg (flow of 50  $nL\ min^{-1}$ ). All perfusion experiments were performed within 120 min after sacrifice of mice. The tone of afferent arterioles

was tested by rapidly increasing the perfusion pressure and assessing the change in the luminal diameter. A fast and complete constriction in response to KCl (100 mmol L<sup>-1</sup>) solution was used as a criterion to identify the suitability of afferent arterioles for the subsequent experiments. This test was repeated at the end of the experiment. Only arterioles with full constriction were accepted. After a 10 min stabilization period at 37 °C, experiments were begun. The perfused arterioles were continuously recorded in digital movies using a digital video disc recorder attached to the microscope's camera. The perfusate was then exchanged with BSA (30 mg mL<sup>-1</sup>), Hb (30 mg mL<sup>-1</sup>), APs, and HbPs (each 10% by volume corresponding to a protein content of 30 mg mL<sup>-1</sup>) for 11 min. Finally, angiotensin II (Sigma, Hamburg, Germany) was applied in the bath to obtain a concentration-response curve (10<sup>-12</sup> to 10<sup>-6</sup> mol L<sup>-1</sup>) with 2 min intervals for each concentration. Digital pictures were serially acquired from the digital movie for each experiment and were used to measure arteriolar luminal diameter. In all series, the last 15 s of each interval was used for statistical analysis of steady-state responses. The data are presented as absolute diameters ( $\mu$ m) and relative values, *i.e.*, percentage (%) of the initial diameter.

**Statistics.** Results of afferent arteriolar diameter measurements were expressed as means  $\pm$  standard error of the mean. Diameter data were compared using Brunner's test (a nonparametric ANOVA-like test for repeated measurements and multiple comparisons).<sup>38</sup> The test is appropriate for comparison of series of repeated measurements with no normal distribution and was performed by using R (the program "R-environment for statistical computing" may be obtained at [www.r-project.org](http://www.r-project.org)). The functions for running Brunner's test may be obtained at [www.ams.med.uni-goettingen.de/amsneu/longit-de.shtml](http://www.ams.med.uni-goettingen.de/amsneu/longit-de.shtml).  $p < 0.05$  was used to reject the null hypothesis.

**Conflict of Interest:** The authors declare no competing financial interest.

**Supporting Information Available:** Perfusion videos: Perfusion with a concentrated HbP suspension of 10% and reaction of afferent arterioles after angiotensin II addition during the perfusion of the glomerulus with Hb solution and HbPs, respectively. This material is available free of charge *via* the Internet at <http://pubs.acs.org>.

**Acknowledgment.** We thank Dr. Dimitriya Borisova (Max-Planck Institute of Colloids and Interfaces, Golm, Germany) for SEM imaging and Ms. Iris Pieper at TU Berlin for ICP-OES measurements. We acknowledge the financial support of the European Community (EFRE-ProFIT 10139827).

## REFERENCES AND NOTES

1. Funk, M.; Günay, S.; Lohmann, A.; Witzenhausen, C.; Henseler, O. *Paul-Ehrlich-Institut Haemovigilance Report 1997–2008. Assessment of Reports of Serious Adverse Transfusion Reactions*; **2008**; Vol. 49, pp 1–26.
2. Whitaker, B. I.; Schlumpf, K.; Schulman, J.; Green, J. *Report of the US Department of Health and Human Services. The 2009 National Blood Collection and Utilization Survey Report*; U.S. Department of Health and Human Services, Office of the Assistant Secretary for Health: Washington, DC, **2011**.
3. Jahr, J. S.; Sadighi, A.; Doherty, L.; Li, A.; Kim, H. W. Hemoglobin-Based Oxygen Carriers: History, Limits, Brief Summary of the State of the Art, Including Clinical Trials. In *Chemistry and Biochemistry of Oxygen Therapeutics: From Transfusion to Artificial Blood*; Mozzarelli, A.; Bettati, S., Eds.; John Wiley & Sons, Ltd.: New York, 2011; pp 301–316.
4. Chen, J.-Y.; Scerbo, M.; Kramer, G. A Review of Blood Substitutes: Examining the History, Clinical Trial Results, and Ethics of Hemoglobin-Based Oxygen Carriers. *Clinics (São Paulo)* **2009**, 64, 803–813.
5. World Health Organization. *Blood Safety: Key Global Fact and Figures in 2011*; **2011**.
6. Chang, T. M. S. Blood Substitutes Based on Nanobiotechnology. *Trends Biotechnol.* **2006**, 24, 372–377.

7. Winslow, R. M. Red Cell Substitutes. *Semin. Hematol.* **2007**, *44*, 51–59.
8. Riess, J. G. Oxygen Carriers ("Blood Substitutes") Raison d'Etat, Chemistry, and Some Physiology Blut Ist Ein Ganz Besonderer Saft. *Chem. Rev.* **2001**, *101*, 2797–2920.
9. Winslow, R. M. Current Status of Blood Substitute Research: Towards a New Paradigm. *J. Intern. Med.* **2003**, *253*, 508–517.
10. Palmer, R. M.; Ferrige, A. G.; Moncada, S. Nitric Oxide Release Accounts for the Biological Activity of Endothelium-Derived Relaxing Factor. *Nature* **1987**, *327*, 524–526.
11. Ignarro, L. J. Endothelium-Derived Relaxing Factor Produced and Released from Artery and Vein Is Nitric Oxide. *Proc. Natl. Acad. Sci. U.S.A.* **1987**, *84*, 9265–9269.
12. Cabrales, P.; Sun, G.; Zhou, Y.; Harris, D. R.; Tsai, A. G.; Intaglietta, M.; Palmer, A. F. Effects of the Molecular Mass of Tense-State Polymerized Bovine Hemoglobin on Blood Pressure and Vasoconstriction. *J. Appl. Physiol.* **2009**, *107*, 1548–1558.
13. Sakai, H.; Hara, H.; Yuasa, M.; Tsai, A. G.; Takeoka, S.; Tsuchida, E.; Intaglietta, M. Molecular Dimensions of Hb-Based O<sub>2</sub> Carriers Determine Constriction of Resistance Arteries and Hypertension. *Am. J. Physiol. Heart Circ. Physiol.* **2000**, *279*, H908–H915.
14. Tabata, Y.; Ikada, Y. Effect of the Size and Surface Charge of Polymer Microspheres on Their Phagocytosis by Macrophage. *Biomaterials* **1988**, *9*, 356–362.
15. Rude, S.; Müller, R. H. *In Vitro* Phagocytosis Assay of Nano- and Microparticles by Chemiluminescence. III. Uptake of Differently Sized Surface-Modified Particles, and Its Correlation to Particle Properties and *in Vivo* Distribution. *Eur. J. Pharm. Sci.* **1993**, *1*, 31–39.
16. Champion, J. A.; Walker, A.; Mitragotri, S. Role of Particle Size in Phagocytosis of Polymeric Microspheres. *Pharm. Res.* **2008**, *25*, 1815–1821.
17. Tong, W.; Song, X.; Gao, C. Layer-by-Layer Assembly of Microcapsules and Their Biomedical Applications. *Chem. Soc. Rev.* **2012**, *41*, 6103–6124.
18. Petrov, A. I.; Volodkin, D. V.; Sukhorukov, G. B. Protein-Calcium Carbonate Coprecipitation: A Tool for Protein Encapsulation. *Biotechnol. Prog.* **2005**, *21*, 918–925.
19. Volodkin, D. V.; Larionova, N. I.; Sukhorukov, G. B. Protein Encapsulation via Porous CaCO<sub>3</sub> Microparticles Templating. *Biomacromolecules* **2004**, *5*, 1962–1972.
20. Tong, W.; She, S.; Xie, L.; Gao, C. High Efficient Loading and Controlled Release of Low-Molecular-Weight Drugs by Combination of Spontaneous Deposition and Heat-Induced Shrinkage of Multilayer Capsules. *Soft Matter* **2011**, *7*, 8258–8265.
21. Tong, W.; Gao, C. Multilayer Microcapsules with Tailored Structures for Bio-Related Applications. *J. Mater. Chem.* **2008**, *18*, 3799–3812.
22. Xiong, Y.; Steffen, A.; Andreas, K.; Müller, S.; Sternberg, N.; Georgieva, R.; Bäumler, H. Hemoglobin-Based Oxygen Carrier Microparticles: Synthesis, Properties, and *In Vitro* and *In Vivo* Investigations. *Biomacromolecules* **2012**, *13*, 3292–3300.
23. Bäumler, H.; Georgieva, R. Coupled Enzyme Reactions in Multicompartment Microparticles. *Biomacromolecules* **2010**, *11*, 1480–1487.
24. Mak, W. C.; Georgieva, R.; Renneberg, R.; Bäumler, H. Protein Particles Formed by Protein Activation and Spontaneous Self-Assembly. *Adv. Funct. Mater.* **2010**, *20*, 4139–4144.
25. Lee, K.; Choi, S.; Yang, C.; Wu, H.-C.; Yu, J. Autofluorescence Generation and Elimination: A Lesson from Glutaraldehyde. *Chem. Commun.* **2013**, *49*, 3028–3030.
26. Zuckerman, K. S. Approach to the Anemias. In *Cecil Medicine*; Goldman, L.; Ausiello, D. A., Eds.; Saunders Elsevier: Philadelphia, PA, 2007.
27. Linberg, R.; Conover, C. D.; Shum, K. L.; Shorr, R. G. Hemoglobin Based Oxygen Carriers: How Much Methemoglobin Is Too Much? *Artif. Cells, Blood Substitutes, Biotechnol.* **1998**, *26*, 133–148.
28. Patzak, A.; Steege, A.; Lai, E. Y.; Brinkmann, J. O.; Kupsch, E.; Spielmann, N.; Gericke, A.; Skalweit, A.; Stegbauer, J.; Persson, P. B.; et al. Angiotensin II Response in Afferent Arterioles of Mice Lacking Either the Endothelial or Neuronal Isoform of Nitric Oxide Synthase. *Am. J. Physiol. Regul. Integr. Comp. Physiol.* **2008**, *294*, R429–R437.
29. Patzak, A.; Lai, E.; Persson, P. B.; Persson, A. E. G. Angiotensin II–Nitric Oxide Interaction in Glomerular Arterioles. *Clin. Exp. Pharmacol. Physiol.* **2005**, *32*, 410–414.
30. Patzak, A.; Mrowka, R.; Storch, E.; Hocher, B.; Persson, P. B. Interaction of Angiotensin II and Nitric Oxide in Isolated Perfused Afferent Arterioles of Mice. *J. Am. Soc. Nephrol.* **2001**, *12*, 1122–1127.
31. Ito, S.; Johnson, C. S.; Carretero, O. A. Modulation of Angiotensin II-Induced Vasoconstriction by Endothelium-Derived Relaxing Factor in the Isolated Microperfused Rabbit Afferent Arteriole. *J. Clin. Invest.* **1991**, *87*, 1656–1663.
32. Thompson, A.; McGarry, A. E.; Valeri, C. R.; Lieberthal, W. Stroma-Free Hemoglobin Increases Blood Pressure and GFR in the Hypotensive Rat: Role of Nitric Oxide. *J. Appl. Physiol.* **1994**, *77*, 2348–2354.
33. Reid, T. J. Hb-Based Oxygen Carriers: Are We There Yet? *Transfusion* **2003**, *43*, 280–287.
34. Haney, C. R.; Buehler, P. W.; Gulati, A. Purification and Chemical Modifications of Hemoglobin in Developing Hemoglobin Based Oxygen Carriers. *Adv. Drug Delivery Rev.* **2000**, *40*, 153–169.
35. Zijlstra, W. G.; Buursma, A. Spectrophotometry of Hemoglobin: Absorption Spectra of Bovine Oxyhemoglobin, Deoxyhemoglobin, Carboxyhemoglobin, and Methemoglobin. *Comp. Biochem. Physiol., Part B: Biochem. Mol. Biol.* **1997**, *118B*, 743–749.
36. Zhang, X.; Liu, C.; Yuan, Y.; Shan, X.; Sheng, Y.; Xu, F. A Noninvasive Method for Measuring the Oxygen Binding-Releasing Capacity of Hemoglobin-Loaded Polymeric Nanoparticles as Oxygen Carrier. *J. Mater. Sci.: Mater. Med.* **2009**, *20*, 1025–1030.
37. Patzak, A.; Lai, E. Y.; Mrowka, R.; Steege, A.; Persson, P. B.; Persson, A. E. G. AT1 Receptors Mediate Angiotensin II-Induced Release of Nitric Oxide in Afferent Arterioles. *Kidney Int.* **2004**, *66*, 1949–1958.
38. Brunner, E.; Puri, M. L. Nonparametric Methods in Factorial Designs. *Stat. Pap.* **2001**, *42*, 1–52.